Crystal Structures of the Fluorinated Fullerenes $C_{60}F_{36}$ and $C_{60}F_{48}$

S. Kawasaki,* T. Aketa, H. Touhara, and F. Okino

Faculty of Textile Science and Technology, Shinshu University, Ueda 386-8567, Japan

O. V. Boltalina, I. V. Gol'dt, and S. I. Troyanov

Chemistry Department, Moscow State University, 119899 Moscow, Russia

R. Taylor

The Chemistry Laboratory, CPES School, University of Sussex, Brighton BN1 9QJ, U.K.

Received: August 18, 1998; In Final Form: October 13, 1998

To elucidate the structures of $C_{60}F_{36}$ and $C_{60}F_{48}$, X-ray diffraction and electron diffraction experiments have been performed. It was found that the X-ray diffractograms of $C_{60}F_{36}$ and $C_{60}F_{48}$ at room temperature are indexed by bcc and bct lattices, respectively. In situ X-ray diffraction experiments at high temperatures have been also undertaken. The bct to fcc phase transition of $C_{60}F_{48}$ was observed. The mechanism of the transition and the stabilities of the structures of fluorinated fullerenes are discussed.

Introduction

Since fluorinated fullerenes, $C_{60}F_x$, have elegant molecular structures and are expected to be applied for new functionality materials, they are among the most attractive materials from both crystallographic and industrial points of view. Although many researchers have characterized fluorinated fullerenes,[1] there still remain ambiguities due to the difficulty in producing fluorinated fullerenes of specific fluorine contents. Recently, Boltalina et al.[2−6] and Gakh et al.[7] reported the synthesis of high-purity $C_{60}F_{18}$, $C_{60}F_{36}$, and $C_{60}F_{48}$. They also investigated the molecular structures by using ^{19}F NMR. However, the crystallographic studies have so far been limited to the samples of unpurified $C_{60}F_x$,[8−10] where only the average value of x was known. Since high-purity $C_{60}F_{36}$ and $C_{60}F_{48}$ have now become available, we have performed X-ray diffraction and electron diffraction experiments on these samples. The structural changes at high temperatures were also investigated by in situ high-temperature X-ray experiments.

Experimental Section

Samples, $C_{60}F_{36}$ and $C_{60}F_{48}$, were synthesized by the methods described elsewhere.[3,4,6]

To confirm the fluorine contents and the homogeneity of the samples, we performed mass spectroscopic measurements and X-ray photoelectron spectroscopic (XPS) measurements. Field-desorption mass spectra (FD-MS) were taken on a Hitachi M80B. C_6F_6 was used as the solvent. The emission voltage and current were 8−10 kV and 40 mA, respectively. XPS measurements were done on an Ulvac-phi model 5600 using non-monochromatic Mg Kα X-rays at 1253.6 eV. The XPS spectra were observed at pressures below 10^{-9} Torr.

Powder X-ray diffraction (XRD) and electron diffraction experiments were undertaken to investigate the crystal structures. XRD measurements were performed on a Rigaku RINT-2200 using Cu Kα radiation. Pyrolytic graphite was used as a counter monochromator. The powder was sealed in a 0.2 mm diameter silica glass capillary. High-temperature experiments were done with a handmade small furnace consisting of a 10 mm diameter ceramic tube wound by a Pt wire with windows for incident and diffracted beams. The sample in the capillary was set in the furnace. The sample temperature was monitored by a thermocouple on the top of the furnace. The distance from the sample to the thermocouple was about 20 mm. Prior to the experiments, the sample temperature was calibrated by setting an extra thermocouple at the sample position. Electron diffraction measurements were performed for $C_{60}F_{36}$ with a JEOL JEM-2010 electron microscope. The accelerating voltage was set at 200 kV.

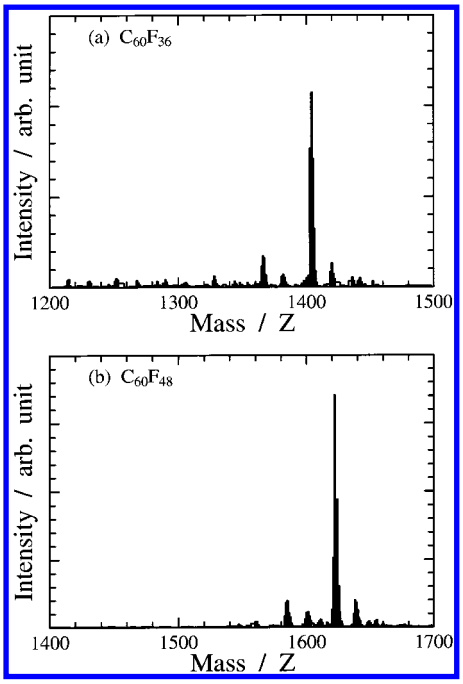

Figure 1. Observed mass spectra of (a) $C_{60}F_{36}$ and (b) $C_{60}F_{48}$.

Results and Discussion

Figure 1 shows the observed FD-MS mass spectra of $C_{60}F_{36}$ and $C_{60}F_{48}$. It was confirmed that $C_{60}F_{36}$ and $C_{60}F_{48}$ are the

10.1021/jp983394d CCC: $18.00
Published on Web 02/06/1999

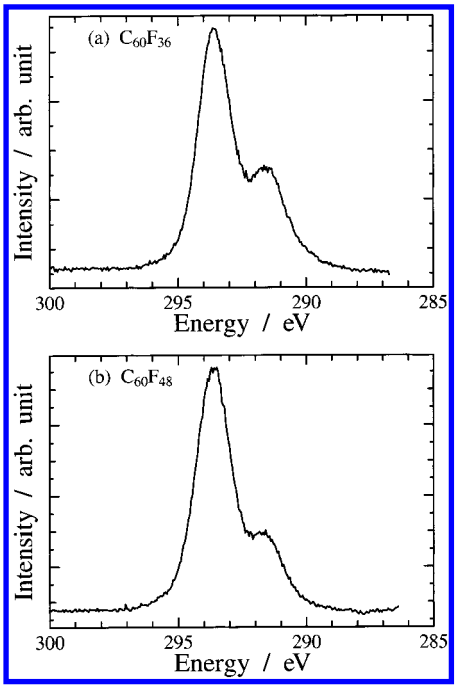

Figure 2. Observed XPS spectra of (a) $C_{60}F_{36}$ and (b) $C_{60}F_{48}$.

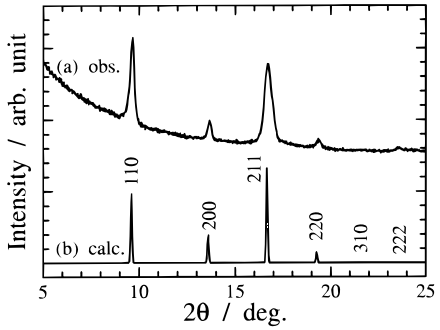

Figure 3. (a) Observed and (b) simulated XRD spectra of $C_{60}F_{36}$.

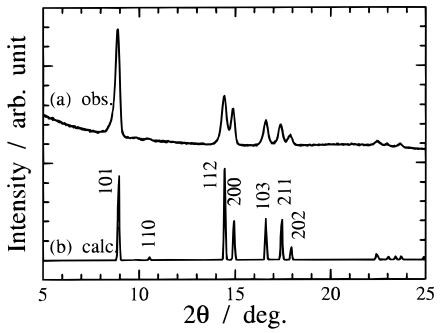

Figure 4. (a) Observed and (b) simulated XRD spectra of $C_{60}F_{48}$.

main products. Figures 2 shows the observed C 1s XPS spectra of $C_{60}F_{36}$ and $C_{60}F_{48}$. There are two features in both spectra; the higher and lower energy features correspond to C 1s of carbon atoms attached to fluorine atoms and of bare carbon atoms, respectively. The ratios of the integrated intensities of these two features for $C_{60}F_{36}$ and $C_{60}F_{48}$ are consistent with the main components detected by mass analyses. Figures 3a and 4a show the observed XRD diagrams of $C_{60}F_{36}$ and $C_{60}F_{48}$, respectively. In our previous powder XRD studies using $C_{60}F_x$ ($x \simeq 45-46$) samples, the structure was determined to be fcc.[8−10] In this study, however, we found that neither $C_{60}F_{36}$ nor $C_{60}F_{48}$ has an fcc structure at room temperature. There seem to be mainly chemical reasons for the previous fcc assignment

Figure 5. Selected area electron diffraction photograph of $C_{60}F_{36}$.

TABLE 1: Lattice Parameters, *Z*, and *V*/*Z*

	lattice parameters (nm)			
	a	*c*	*Z*	*V*/*Z* (nm^3)
$C_{60}F_{36}$ (bcc)	1.302(1)		2	1.104
$C_{60}F_{48}$ (bct)	1.1852(8)	1.791(1)	2	1.257
$C_{60}F_x$ (fcc)	1.7158(3)		4	1.263

of the $C_{60}F_x$ samples; the variation in the number of fluorine atoms from molecule to molecule favors an average fcc molecular arrangement, whereas the presence of a single molecular species in the $C_{60}F_{36}$ and $C_{60}F_{48}$ samples brings about lowering of the lattice symmetry to bcc and bct, respectively.

The electron diffraction spots in Figure 5, which are the lowest angle diffractions of $C_{60}F_{36}$, show 6-fold rotational symmetry. The lowest diffraction of the fcc structure is 111 and cannot have such symmetry. It was found that the XRD diffraction lines of $C_{60}F_{36}$ can be indexed by a bcc lattice. The lowest diffraction of bcc is 110 and has 6-fold rotational symmetry.

On the other hand, the diffraction pattern of $C_{60}F_{48}$ is rather complicated in comparison with that of $C_{60}F_{36}$. The pattern can no longer be indexed by a cubic lattice. To index all the diffraction lines, a tetragonal unit cell needs to be used. Furthermore, the extinction rule found in the XRD diagram indicates that the unit cell of $C_{60}F_{48}$ is *I*-centered tetragonal (bct).

Table 1 summarizes the lattice parameters, number of molecules (*Z*) in a unit cell, and volume per molecule (*V*/*Z*) of $C_{60}F_{36}$ and $C_{60}F_{48}$ powder samples and a $C_{60}F_x$ ($x \simeq 46$) single crystal.[10]

The difference in *V*/*Z* values between $C_{60}F_{48}$ and $C_{60}F_x$ is small, suggesting the structural similarity of the two structures. The extended bct cell can be treated as a face centered tetragonal ("fct") cell which is derived by the elongation of an fcc cell along the *c* axis with the new choice of *a* axis coinciding with the *C* face diagonal of the initial bct cell. Indeed, the lattice parameters of this extended "fct" cell for $C_{60}F_{48}$ are $a = 1.675$ nm and $c = 1.79$ nm, which are close to the lattice constant $a = 1.716$ nm of $C_{60}F_x$, confirming the close structural resemblance of these two materials.

It is interesting to note that the volume per molecule for $C_{60}F_x$ is slightly larger than that for $C_{60}F_{48}$, despite the facts that the average number of fluorine atoms in $C_{60}F_x$ ($x \simeq 46$) is smaller than 48 and that the fcc structure ought to be denser than the bct structure based on the simple hard-sphere model. As mentioned above, the irregularity in size and shape among the $C_{60}F_x$ molecules together with the thermal motion can make them assume maximal spherical size in comparison with the

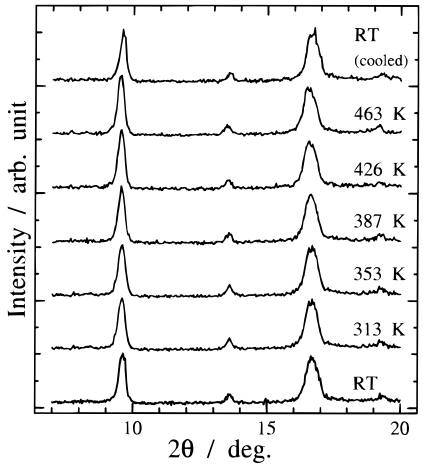

Figure 6. Change in XRD diffraction pattern of $C_{60}F_{36}$ with temperature.

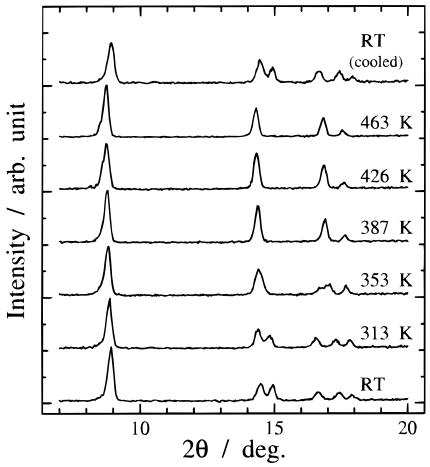

Figure 7. Change in XRD diffraction pattern of $C_{60}F_{48}$ with temperature.

case of $C_{60}F_{48}$. (See also the discussion below on the phase transition of $C_{60}F_{48}$.)

We tried to simulate the observed diffraction patterns by using bcc and bct model structures for $C_{60}F_{36}$ and $C_{60}F_{48}$, respectively. First, we describe the model for $C_{60}F_{48}$. We previously elucidated by single-crystal X-ray analysis[10] that the randomly rotating $C_{60}F_x$ molecule can be expressed by three atomic shells: two carbon atom shells having the radii of 0.31 and 0.38 nm and one fluorine atom shell of radius 0.51 nm. The molecule of $C_{60}F_{48}$ is considered not to be much different from that of $C_{60}F_x$. However, the three-shell model is too sophisticated to deal with the limited numbers of diffraction peaks observed in the powder XRD pattern. Therefore, two shells (one fluorine and one carbon atom shell) were used to simplify the model. The radii r_F and r_C of the fluorine and carbon atom shells were set equal to 0.51 and 0.37 nm, respectively.

A two-shell model with $r_F = 0.49$ nm and $r_C = 0.35$ nm was used for $C_{60}F_{36}$.

Figures 3 and 4 show the simulated and observed diffraction diagrams. As shown in Figures 3 and 4, both simulations reproduce the observed diagrams well. It was found that the calculated intensity of the 110 diffraction of $C_{60}F_{48}$, which is allowed by the extinction rule, is very weak in accordance with the observed pattern. The disagreement between the calculated and observed intensities in the higher angle region could be explained by the nonspheric distribution of electrons in the real molecules despite the thermal motion.

Figures 6 and 7 show the change in the diffraction patterns of $C_{60}F_{36}$ and $C_{60}F_{48}$ with temperature. As shown in Figure 6, no remarkable change was observed in the diagrams of $C_{60}F_{36}$. On the other hand, the diffraction pattern of $C_{60}F_{48}$ begins to change at about 353 K (Figure 7). The phase at high temperatures is fcc. This bct to fcc transition of $C_{60}F_{48}$ is reversible since the sample after the high temperature measurements showed the same pattern as that of the starting sample. As mentioned in the previous paragraph, the bct cell of $C_{60}F_{48}$ can be expressed as an extended "fct" cell which is a modified fcc cell. The a/c ratio of the extended "fct" cell becomes closer to 1 with increasing temperature and exactly 1 at the transition temperature.

We speculate the mechanism of this transition as follows. The molecular structure of $C_{60}F_{48}$ is known as D_3 symmetry on the basis of the NMR spectrum.[7] Provided that all the unique axes of the molecules lie parallel to the c axis of the bct cell and that the molecules rotate around these axes, the a/c ratio should be different from 1. However, at high temperature, the more vigorous and random motion of the molecules will make the apparent molecular shape spherical and the fcc phase can appear. On the other hand, two isomers are known for $C_{60}F_{36}$ molecules having T and C_3 symmetries.[5] The bcc crystal structure may have arisen owing to the T symmetry of the molecule, which belongs to the cubic group, coupled with thermal motion. Mixing of the C_3 molecules can randomize molecular orientations, resulting in an apparent spherical shape on average. At this stage, however, no definitive conclusion can be drawn since the ratio of the T and C_3 isomers of the samples used in this study was not clearly known.

It was found that the fcc phase is the stable phase of $C_{60}F_{48}$ at high temperature. Furthermore, the lattice constant of the fcc phase at about 463 K is determined to be 1.72 nm, which is close to the value of the $C_{60}F_x$ ($x \simeq 46$) single crystal (1.716 nm).[10] These results indicate that the fcc single crystal is a metastable phase quenched from high temperature.

Acknowledgment. This work was supported in part by a Grant-in-Aid for Scientific Research (C) (No. 08640643) from the Ministry of Education, Science and Culture of Japan and by a Research for the Future Program of the Japan Society for the Promotion of Science (JSPS-RFTF 96R11701). We thank Mr. A. S. Zapol'skii and Dr. V. K. Pavlovich for preparation of the samples.

References and Notes

(1) Hope, E. G.; Holloway, J. H. *The chemistry of fullerenes*; World Scientific: Singapore, 1995; see also references therein.

(2) Boltalina, O. V.; Markov, V. Y.; Taylor, R.; Waugh, M. P. *Chem. Commun.* **1996**, 2549.

(3) Boltalina, O. V.; Borschevskii, A. Y.; Sidorov, L. N.; Street, J. M.; Taylor, R. *Chem. Commun.* **1996**, 529.

(4) Boltalina, O. V.; Bagryantsev, V. F.; Seredenko, V. A.; Sidorov, L. N.; Zapolskii, A. S.; Taylor, R. *J. Chem. Soc., Perkin Trans. 2* **1996**, 2275.

(5) Boltalina, O. V.; Street J. M.; Taylor, R. *J. Chem. Soc., Perkin Trans. 2* **1998**, 649.

(6) Boltalina, O. V.; Gol'dt, I.; Zatsepin, T.; Spiridonov, F. M.; Troyanov, S. I.; Sidorov, L. N.; Taylor, R. *Molecular Nanostructures. Proceedings of the International Winter School on Electronic Properties of Novel Materials*; World Scientific: Singapore, 1998; p 114.

(7) Gakh, A. A.; Tuinman, A. A.; Adcock, J. L. *J. Am. Chem. Soc.* **1994**, *116*, 819.

(8) Okino, F.; Touhara, H.; Seki, K.; Mitsumoto, R.; Shigematsu, K.; Achiba, Y. *Fullerene Sci. Technol.* **1993**, *1*, 425.

(9) Okino, F.; Fujimoto, H.; Ishikawa, R.; Touhara, H. *Trans. Mater. Res. Soc. Jpn.* **1994**, *14*, 1205.

(10) Okino, F.; Kawasaki, S.; Fukushima, Y.; Kimura, M.; Nakajima, T.; Touhara, H. *Fullerene Sci. Technol.* **1996**, *4*, 873.